Semiconductor Physics, Quantum Electronics & Optoelectronics, 2025. V. 28, No 4. P. 464-472.

Optics

Optical and light-emitting properties of silicon nanostructures based on SiO_x films modified with samarium

K.V. Michailovska*, P.E. Shepeliavyi, V.K. Lytvyn, O.V. Dubikovskyi, V.A Dan'ko, I.Z. Indutnyi, M.V. Sopinskyy

V. Lashkaryov Institute of Semiconductor Physics, NAS of Ukraine, 45 Nauky Avenue, 03028 Kyiv, Ukraine
**Corresponding author e-mail: k_mich@ukr.net*

Abstract. The composition, optical and luminescent properties of SiO_x:Sm films prepared by vacuum thermal evaporation of a powder mixture of SiO + 1 wt.% Sm have been studied. The study of elemental profiles by time-of-flight secondary ion mass spectroscopy revealed an almost uniform depth distribution of the major elements (Si and O, tracked by presence of Si^+, Si_2^+, O^+ and SiO^+ ions) as well as Sm (tracked by presence of Sm^+ and SmO^+ ions). Infrared absorptance spectra ($A = 1 - R - T$) showed a greater microstructural heterogeneity of the SiO_x matrix in the studied films as compared to undoped SiO_x films obtained in a similar deposition regime. Further heat treatment in vacuum at 500…700 °C increases the heterogeneity degree of the samples. The optical band gap values of the SiO_x:Sm films of 1.5 eV before and 1.77 eV after annealing at 600 °C, determined by the Tauc method correlate well with the literature data for amorphous silicon and Si nanoinclusions in SiO_2 matrix, respectively. Measurements of photoluminescence spectra and their analysis have shown that doping of SiO_x films with samarium stimulates their decomposition, and heat treatments at temperatures ≥ 600 °C forms Si nanoparticles in an oxide matrix that exhibit a quantum-size effect.

Keywords: silicon nanoparticles, SiO_x, nanocomposite, samarium, rare-earth elements, lanthanoids, luminescence.

https://doi.org/10.15407/spqeo28.04.464
PACS 78.30.Am, 78.60.Lc, 78.66.-w, 78.67.Bf, 78.67.-n

Manuscript received 20.05.25; revised version received 03.11.25; accepted for publication 26.11.25; published online 15.12.25.

1. Introduction

Properties of nanoscale silicon structures have been a focus of extensive research over the past three decades. Thin-film silicon-silicon oxide nanocomposites (nps-Si–SiO_x), where nps-Si are amorphous or crystalline silicon nanoparticles, are considered to be quite promising. The motivation for studying these structures stems from their potential applications in various fields, including optoelectronic devices, non-volatile memory devices, and solar energy technologies [1–9]. The key factor in the wide use of these materials is the ability to modify their structural, optical, luminescent and other properties during the manufacturing process [10–14].

Introduction of ions of rare-earth elements (lanthanoids (Ln): Ce, Er, Eu, Tb, Sm, *etc*.) significantly expands use of these nanocomposites in modern photonics, optoelectronics, photovoltaics, *etc*. [1–3]. This explains the scientific interest in studying influence of Ln impurities on formation of nps-Si in an oxide matrix and the role of the ncs-Si as sensitizers for Ln^{3+} ions, especially Er^{3+}. It was demonstrated in particular that the Er impurity has a stimulatory effect on nucleation and growth of Si nanocrystals during heat treatment of SiO_x:Er films deposited by reactive sputtering in an Ar/O_2 atmosphere [15] and magnetron co-sputtering [16]. The authors of [17, 18] found that air annealing of SiO_x:Er,F films obtained by co-evaporation of SiO and ErF_3 leads to more intense crystallization of amorphous ncs-Si and formation of a more perfect oxide matrix structure compared to those in SiO_x films obtained by evaporation of SiO and undergone similar annealing.

Nanosilicon thin-film structures doped with samarium ions are poorly studied compared to *e.g.* erbium-doped ones. Meanwhile, phosphorescence of samarium-doped silicate glasses has long been studied and is widely used in fiber-optic communication devices, white light-emitting diodes (w-LEDs) [19], ionizing radiation dosimeters [20], *etc*. Recently, photo-luminescence of samarium-doped SiO_x films containing Si nanoparticles has been studied [21–23]. It has been demonstrated in [21] that in the films obtained

by co-evaporation of SiO and metallic Sm in vacuum, formation of light-emitting crystalline silicon nanoparticles occur at lower annealing temperatures compared to SiO_x films without samarium. In [22], SiO_x films doped with samarium were obtained by annealing a multilayer structure $(SiO_x/Sm)_n$. This structure comprised pairs of thin layers of SiO_x and Sm. In such structures, the samarium dopant promoted decomposition of SiO_x into Si and SiO_2 as well as crystallization of Si nanoparticles. The crystallization was observed even at 750 °C. At this annealing temperature, the relative volume fraction of the nanocrystals in the silicon phase was found to be approximately 38%. It is nearly double the amount observed in samples obtained by co-evaporation with subsequent annealing at 970 °C.

This paper presents the results of comprehensive studies of SiO_x:Sm films obtained by thermal evaporation of a (SiO+Sm) powder mixture from a single evaporator, followed by heat treatment. The aim of the work is to study the possibilities of creating light-emitting nanostructures based on SiO_x:Sm films obtained using this simple technology as well as to determine the effect of samarium on the film structural, optical, and luminescent properties.

2. Materials and methods

The investigated SiO_x:Sm films were prepared by thermal evaporation in a vacuum of ~10^{-3} Pa of a mixture of SiO (Cerac Inc., Milwaukee, WI, USA, purity of 99.9%) and Sm (~1 wt.%) powders in a closed-type molybdenum evaporator with a small hole in the center. The films were deposited onto HF-treated double-side polished c-Si substrates heated to 100 °C and fused quartz substrates. The deposition rate was controlled *in situ* using a quartz thickness gauge KIT-1. The thickness of the resulting films was measured with a microinterferometer MII-4 to be 350 nm. To form nanosized silicon, the samples were annealed in a vacuum chamber at temperatures T_{an} = 500…700 °C for 15 min. During heat treatment, along with phase decomposition of the films, passivation of broken silicon bonds on the surface of the formed nanoinclusions occurred due to interaction with the atmosphere of residual gases. The formation of Si–O–Sm, Si–O (or Si=O) bond types was detected by the appearance of stable in time luminescence from the annealed samples as well as by their infrared absorption spectra.

The elemental composition and its distribution over the film depth were studied by time-of-flight secondary ion mass spectrometry (TOF-SIMS) using an Ion TOF SIMS IV spectrometer (ION TOF Inc, Chestnut Hill, NY, USA) by sputtering the sample surface with Cs^+ ions at an energy of 2000 eV for 500 s. Absorption of the films on c-Si substrates in the infrared spectral region was studied using a PerkinElmer BXII spectrometer with a resolution of 4 cm^{-1}. The contribution of an uncoated reference silicon substrate was subtracted from the measured film spectra.

Optical properties of the SiO_x:Sm films were investigated on the samples deposited onto fused quartz substrates. Light transmittance spectra were measured in the spectral range of 390 to 850 nm with a step of 0.5 nm using a ScanSpec UV-Vis spectrometer on a diffraction grating (600 lines/mm) and a CCD matrix (Sony ILX 511). A halogen incandescent lamp was used as the light source. The setup for measuring reflectance included the same light source, an optical system for forming an incident light beam based on a set of apertures and an 8× objective, and a sample holder mounted on a two-axis table. The optical system for recording the reflected light included an optical waveguide with a core diameter of 1 mm and a radiation receiver consisting of a spectrometer and a matrix. The signal reflected from a silver mirror of the same thickness as the substrate of the samples was used as the reference signal for measuring the reflectance spectra.

Photoluminescence (PL) was excited by a LED laser emitting at a wavelength of 405 nm. A CC-8 filter was used to block the background LED radiation in the range of 500 to 1500 nm. The excitation light was modulated by a mechanical modulator with a frequency of 110 Hz. A ZMR-3 monochromator and a liquid nitrogen cooled FEU-62 photomultiplier tube connected to a 232B synchronous nanovoltmeter (Unipan) were used to record the PL signal. The spectral sensitivity of the setup was taken into account while analyzing the measured PL spectra.

3. Results and discussion

The yield of secondary monatomic and polyatomic ions was measured as a function of sputtering time. Presence of Si^+, Si_2^+, O^+, SiO^+ ions, as well as Sm^+ and SmO^+ ions was recorded. Fig. 1 shows the distribution profiles of these ions obtained by sputtering of a SiO_x:Sm film annealed at 600 °C. These profiles show that the film has a rather uniform elemental composition over the depth, except for the film/Si substrate interface.

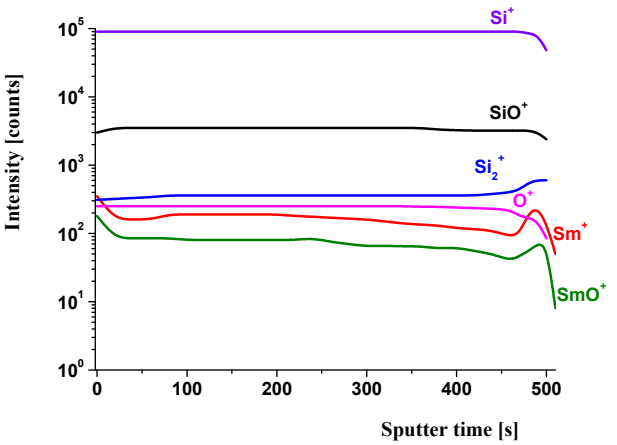

Fig. 1. Distribution profiles of monoatomic and polyatomic ions as functions of sputtering time of a SiO_x:Sm film annealed at 600 °C in vacuum for 15 min.

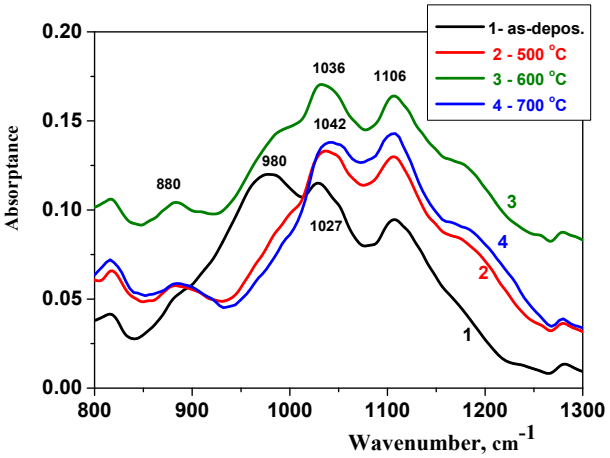

Fig. 2. IR absorptance spectra of SiO_x:Sm films before (*1*) and after annealing in vacuum at 500 (*2*), 600 (*3*), and 700°C (*4*) during 15 min.

The thickness of the region with a non-uniform element distribution was <10% of the total film thickness of ~350 nm.

In order to study the structure of the SiO_x:Sm film matrix and its changes during thermally stimulated phase transformations, infrared (IR) absorptance spectra ($A = 1 - R - T$) in the range of 800 to 1300 cm^{-1} were measured. Transmittance (T) and reflectance (R) were measured at normal light incidence. Fig. 2 shows the absorptance spectra of the SiO_x:Sm films before (curve *1*) and after heat treatment at 500, 600 and 700 °C (curves *2*, *3* and *4*, respectively).

In the spectrum of the deposited film, the most prominent peaks of vibrational modes at 980, 1027, and 1106 cm^{-1} are located in the region of the main absorption band on asymmetric (TO_3) vibrations of bridging oxygen atoms that are part of $Si–O_y–Si_{4-y}$ ($1 \le y \le 4$) molecular complexes of silicon oxide. It is noteworthy that the components of the main vibrational band are discernible without a need to decompose the spectrum into elementary profiles. The appearance of the bands at 980 and 1027 cm^{-1} in the spectrum of the freshly deposited SiO_x:Sm film indicates presence of molecular complexes of weakly oxidized ($SiOSi_3$) and partially oxidized (SiO_2Si_2) silicon. These bands are characteristic of SiO_x ($x < 2$) compositions.

Moreover, the absorptance spectrum contains a band with a maximum at 1106 cm^{-1} corresponding to fully oxidized SiO_4 molecular complexes. The band at 1106 cm^{-1} is usually associated with vibrational modes of SiO_4 tetrahedra in silica interconnected in *n*-member rings ($n \le 6$) [24]. Such rings are formed at large angles of Si–O–Si bonds and are characterized by an increased vibration frequency. Presence of the SiO_2 phase in the as-deposited film is also indicated by a small band at 810 cm^{-1} corresponding to bending vibrations of Si–O–Si bonds in SiO_2 [25]. After annealing at 500 °C, the band at 980 cm^{-1} almost disappears (curve *2*) and the areas under the rest of the bands increase, reaching their maximum values after treatment at 600 °C (curve *3*). The band at 1027 cm^{-1} shifts towards higher wave numbers (1042 cm^{-1}) indicating an increase in the concentration of bridging oxygen atoms and improvement in the stoichiometry of the oxide matrix. The band at 1106 cm^{-1} remains static, thereby confirming its affiliation with the SiO_2 phase.

A plateau in the region of 1150 to 1200 cm^{-1} appears in the IR spectra of the annealed samples. A small band at 880 cm^{-1}, the nature of which has not yet been clearly established, is also observed. For the heat-treated SiO_x films, the band at 880 cm^{-1} was associated with interaction between Si and non-bridging oxygen atoms in SiO_2 [26]. Another study, examining spectra of SiO/SiO_2 multilayer structures annealed at 300…600 °C, attributed the band at 880 cm^{-1} to the configuration of silicon rings isolated by oxygen atoms [27].

It may be concluded from analysis of the vibrational modes shown in Fig. 2 and comparison of them with the vibrational modes of undoped SiO_x and SiO_2 films that the composition of the oxide matrix of the SiO_x:Sm films, both before and after annealing, is inhomogeneous, *i.e.* the matrix consists of a mixture of SiO_x ($x < 2$) and SiO_2 phases. Previous studies of infrared spectra of non-doped SiO_x films deposited in a similar manner but without samarium showed that SiO_2 phase was almost absent. It appeared only after annealing at 1000…1100 °C as a result of thermally stimulated decomposition of the SiO_x films. Hence, interaction between the components of the (SiO + Sm) powder mixture is likely to occur during thermal evaporation, resulting in partial decomposition of SiO. Phase separation of the SiO_x:Sm film enhances during annealing, leading to an increase in the degree of heterogeneity. This is indicated by the appearance of the LO_4 (1160 cm^{-1}) and TO_4 (1200 cm^{-1}) doublets in the 1150…1200 cm^{-1} region in a form of a plateau. Hence, the infrared absorption spectra reveal a significant effect of the evaporation-deposition conditions of SiO and Sm on the microstructure of the deposited SiO_x:Sm films and the thermal budget of the suboxide phase separation. When a mixture of silicon monoxide and samarium powders is heated in a quasi-closed evaporator, chemical interactions between the two substances may occur, which will effect the composition of the resulting vapors. Samarium is an active metal, particularly when it is in a molten or gaseous state. At high temperatures (~1000 °C), which are close to the melting point of Sm and sublimation point of SiO, a reaction such as $3SiO + 2Sm \rightarrow 3Si + Sm_2O_3$, may occur. Such a reaction will lead to appearance of silicon molecular fragments (clusters) and Sm_2O_3 molecules in the depositing vapor phase, which will result in formation of silicon nanoparticles in the deposited film and a significant modification of the matrix. We did not observe any bands characteristic of Sm_2O_3 in the IR spectra in the range of 400 to 600 cm^{-1}, but this may be due to the low atomic

content of Sm in the SiO_x:Sm film. Nevertheless, as can be seen from Fig. 2, the effect of the interaction between samarium and silicon monoxide in the evaporator on the homogeneity of the SiO_x matrix composition is significant. This effect is also confirmed by the optical and luminescent properties of the as-deposited and annealed films.

It should be noted, however, that we did not observe any characteristic lines of electronic transitions in Sm^{2+} and Sm^{3+} ions in the absorption and emission spectra of both the as-deposited and annealed SiO_x:Sm films [28]. The Sm content in the studied films was less than 1.0 at.%. As shown by our previous studies [23], , no emission from Sm^{2+} and Sm^{3+} ions is observed in the PL spectra at such samarium concentration. Moreover, Sm was partially present in the samples in the form of SmO oxide. In cubically symmetric samarium oxide, a local crystal field of high symmetry should act on the samarium ions. In such a situation, no electronic transitions between the absorbing and emitting terms of the Sm ions occur [29, 30]. However, even a small amount of samarium effects the thermally stimulated transformations in SiO_x films.

To study the effect of Sm on the electronic subsystem of the SiO_x films, spectral dependences of the absorption coefficient of the samples on the incident photon energy ($h\nu$) were measured. The formula used for the calculation was as follows:

$$\alpha = \frac{1}{d}\ln\frac{T_s(1-R)}{T}, \qquad (1)$$

where d, T and R are the thickness, transmittance and reflectance of the sample at normal incidence, respectively, and T_s is the transmittance of the quartz substrate.

Fig. 3 shows the spectral dependences of the absorption coefficient of the SiO_x:Sm film in the 1.5…3.2 eV range before and after heat treatment at 600 °C (curves *1* and *2*, respectively). Presence of a band with a maximum at ~1.8 eV at the absorption edge and a non-monotonic increase in α in the region of interband transitions indicate a complex energy structure. A separate paper will be devoted to a detailed analysis of the region below the fundamental absorption edge of SiO_x:Sm films and analysis of the band at 1.8 eV.

The Tauc relation, a common method for estimating the optical band gap (E_{go}) of amorphous materials with $\alpha \geq 10^4$ cm^{-1}, was employed to analyze the data. The Tauc method is also employed in the field of composite materials with nanoinclusions to estimate E_{go} [31]. The band gap width is a pivotal characteristic that facilitates recognition of quantum-size effects in the materials under study. The Tauc theory posits that spectral dependence of allowed interband electronic transitions in semiconductors with an indirect band structure can be represented as follows:

$$\alpha(E) = B\cdot\left(h\nu - E_{go}\right)^2/h\nu, \qquad (2)$$

where B is a coefficient that depends on the probability of the electronic transition [32].

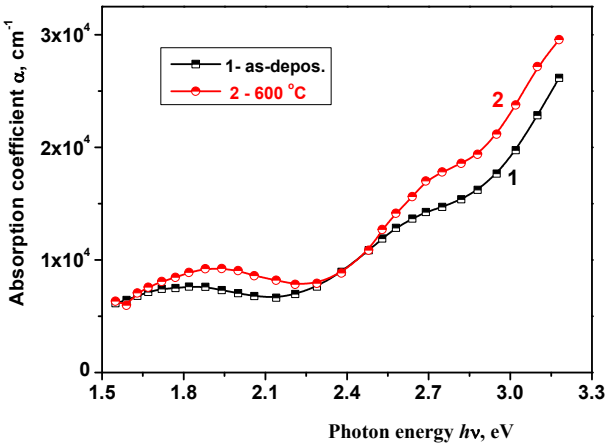

Fig. 3. Spectral dependences of the absorption coefficient of the SiO_x:Sm film before and after heat treatment at 600 °C (curves *1* and *2*, respectively).

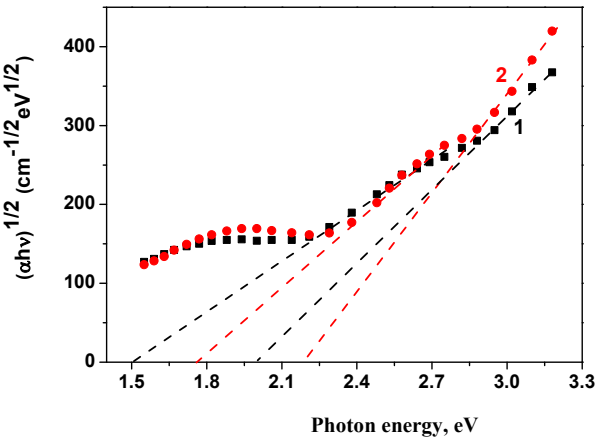

Fig. 4. Spectral dependences of the absorption coefficient in Tauc coordinates of the SiO_x:Sm film before and after heat treatment at 600 °C (curves *1* and *2*, respectively).

Fig. 4 shows the dependence $(\alpha h\nu)^{1/2}$ *versus* $h\nu$ of the SiO_x:Sm film before (*1*) and after (*2*) annealing. The value of E_{go} is determined by the intersection of the linear approximation with the horizontal axis. The film may be considered as a composite with different E_{go} values of its components. Extrapolation of linear approximations with different slopes to $\alpha = 0$ gives an estimation of the E_{go} values of the components that constitute the film.

For the as-deposited film, a linear approximation in the region $h\nu$ = 2.2…2.7 eV yields a value of E_{go} ~ 1.5 eV (Fig. 4, curve *1*). This value of the optical band gap corresponds to the value for defective amorphous nanosilicon phase [33]. The value of E_{go} for silicon nanoparticles depends on their defectivity and size [34]. These two factors act in opposition: the defectivity reduces the E_{go} value and E_{go} increases with decreasing the size of the low-defect *a*-Si nanoparticles. For example, for *a*-Si films, an increase in E_{go} from 1.45 to 1.98 eV was observed as the degree of defectivity decreased [33].

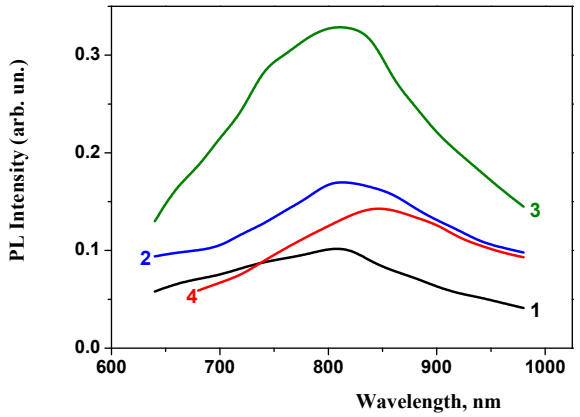

Fig. 5. PL spectra of the SiO_x:Sm film before (*1*) and after annealing at temperatures of 500 (*2*), 600 (*3*) and 700 °C (*4*) in vacuum for 15 min.

For low-defect *a*-Si nanodots in a silicon nitride matrix, the dependence $E_{go} = 2.2/a^2$ (*a* is the nanodot size in nanometers) was observed due to the quantum size effect [34].

In our case, the E_{go} value after annealing the SiO_x:Sm films at 600 °C was determined to be in the same energy range, 1.77 eV (Fig. 4, curve *2*). Since an increase in the size of the a-Si nanoinclusions would be expected during such annealing, the increase in E_{go} from ~ 1.5 to 1.77 eV indicates dominance of reduction in the defectivity of the a-Si inclusions.

As can be seen from Fig. 4, the steepness of the dependence α(*hν*) for the studied samples increases at $h\nu > 2.7$ eV. This is apparently due to the increased influence of the higher E_{go} component, *i.e.* the matrix. The E_{go} values of 2.0 eV before and 2.2 eV after the film annealing were obtained in this region. The increase in the optical band gap is explained by the increase in the matrix stoichiometry index after the annealing, as indicated by the IR spectra. The latter can increase the potential barrier at the nps-Si/matrix interface [35]. This greater barrier increases quantum confinement in the Si nanoparticles, which in turn increases their band gap. Therefore, the increase in E_{go} from 1.5 to 1.77 eV (determined in the energy range $h\nu$ = 2.3…2.7 eV) may not only be due to the reduced defectivity of the ncs-Si, but also due to changes in the surrounding matrix.

The changes in the absorption characteristics are accompanied by changes in the emission characteristics. Fig. 5 shows the PL spectra of the SiO_x:Sm film before (curve *1*) and after vacuum annealing at temperatures of 500, 600 and 700 °C for 15 min (curves *2*, *3*, and *4*, respectively). It can be seen from this figure that the photoluminescence spectrum of the as-deposited film covers the interval from the visible to the near infrared spectral region and PL has a low intensity. To obtain more complete information about the phase transformations of the samples under study, we analyzed their PL spectra by fitting them with Gaussian peaks. Decomposition of the spectrum of the as-deposited film indicates presence of a dominant broad band with a maximum at 800 nm (1.5 eV) (not shown). After annealing at 500 °C, the intensity of this band increases, and its maximum does not change its position (not shown). A similar broad PL band with a maximum at 785 nm was previously observed in SiO_x films annealed at 700 °C [36]. Its appearance was attributed to decomposition of SiO_x and formation of amorphous silicon nanoparticles in an oxide matrix.

Increasing the annealing temperature ($T_{an} \geq 600$ °C) is accompanied by evolution of the emission spectrum. After annealing at 600 °C the integrated PL intensity increases three-fold and the band describing the whole emission spectrum becomes asymmetric and is well approximated by three Gaussian bands with the maxima at 750 nm (1.65 eV), 820 nm (1.51 eV) and 910 nm (1.36 eV) (Fig. 6, curves *1*, *2* and *3*). The presence of the multiple bands in the PL spectrum may indicate different states of structural rearrangement during the phase separation process, in particular, the rearrangement of amorphous silicon nanoinclusions in the SiO_y:Sm ($y > x$) matrix. Previously, qualitative correlation between the emission spectra and the state of the SiO_x phase decomposition in a SiO_x/SiO_2 superlattice was reported in [27].

The sub-oxide deposition technology as well as annealing conditions and temperature have an effect on the size of the formed ncs-Si, their phase state (amorphous, amorphous-crystalline or quasi-crystalline) and the ncs-Si/matrix interface state. These parameters mainly define the mechanism of radiative recombination of carriers corresponding to each specific band. There are several models that explain the mechanism of light emission in nanosilicon structures: (i) excitation and recombination of carriers occur inside the Si nanoparticle; (ii) excitation occurs between quantum levels inside the particle and recombination takes place on the particle surface; and (iii) emission is associated with defects on the nanoparticle surface that form emission levels in the band gap.

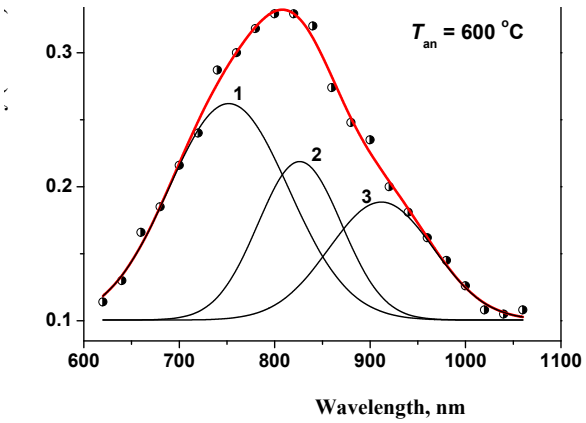

Fig. 6. PL spectrum of the SiO_x:Sm film after vacuum annealing at a temperature of 600 °C for 15 min (dots) and its decomposition into Gaussian components. The red line is the result of superposition of the Gaussian curves *1*, *2* and *3*.

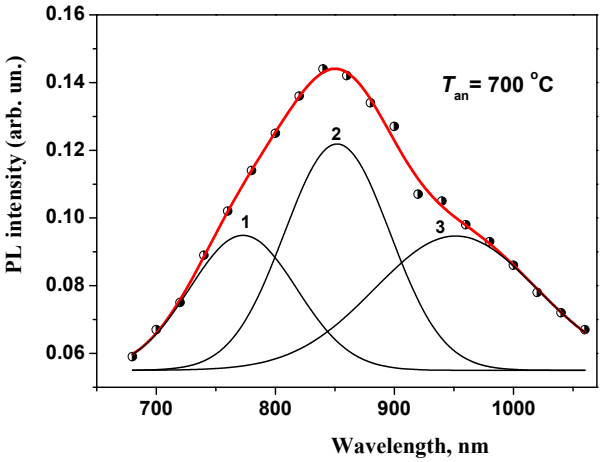

Fig. 7. PL spectrum of the SiO_x:Sm film after vacuum annealing at a temperature of 700 °C for 15 min (dots) and its decomposition into Gaussian components. The red line is the result of superposition of the Gaussian curves *1*, *2* and *3*.

Analyzing the PL spectrum shown in Fig. 6, we can see that the energy position of the peak (1.65 eV) of the PL band at 750 nm (curve *1*) is close to the band gap of the Si nanoparticles (1.77 eV). This may indicate that this band is related to the quantum confinement effect. The energy difference between the values 1.77 and 1.65 eV, *i.e.* the Stokes shift, is ~ (0.12±0.01) eV, which corresponds to the energy (~0.13 eV) of Si–O–Si vibrations with a stretching frequency of ~ 1080 cm^{-1}. This indicates involvement of phonons at the interface nps-Si/SiO_y:Sm ($y > x$) in the radiative processes. The important role of phonons was established in [37], where it was shown that coupling between excitons and stretching vibrations dominates luminescence processes in ncs-Si embedded in an oxide matrix. The Si–O–Si vibrations at the nps-Si/SiO_2 interface provide conditions for momentum conservation in radiation processes in indirect band gap materials.

Therefore, in our opinion, the most intense band with a maximum at 750 nm (1.65 eV) in the PL spectrum of the annealed film is due to recombination of excitons within silicon nanoinclusions. The band with a maximum at 820 nm (Fig. 6, curve *2*) is most likely associated with ncs-Si surface defects at the interface with the matrix in which the ncs-Si are embedded. Presence of oxygen vacancies at the nps-Si/SiO_2 interface, which form radiative defects, has been confirmed both theoretically and experimentally [38]. A similar interpretation of the mechanism of recombination of e-h pairs in silicon nanoparticles with a maximum luminescence at ~820 nm has been given in [37].

Along with the bands at 750 and 820 nm, the PL spectrum also contains a band with a maximum at 910 nm, see Fig. 6 (curve *3*). This band has been observed earlier in the PL spectra of SiO_x:Sm films obtained by co-evaporation of SiO and Sm, but only after annealing at 970 °C [21]. Study of Raman spectra showed formation of crystalline Si nanoparticles in these samples along with amorphous ones. The PL band at 910 nm, attributed to the formation of silicon nanocrystals, has also been observed in SiO_x films annealed in an inert atmosphere at $T_{an} \geq 1000$ °C [31]. We assume therefore that the crystalline or quasi-crystalline (having a crystal core) silicon nanoparticles are responsible for the band at 910 nm in Fig. 6 (curve 3). Annealing at 700 °C leads to a noticeable red shift of the band maximum from 910 to 950 nm accompanied by a decrease in the PL intensity, see Fig. 7 (curve *3*). This behavior is well explained by manifestation of the quantum confinement effect due to the increase in the size of nps-Si.

4. Conclusions

During thermal evaporation of a powder mixture (SiO + Sm), the interaction between its components in the evaporator leads to a partial decomposition of the SiO. As a result, the composition of the oxide matrix of the deposited SiO_x:Sm films is inhomogeneous and consists of a mixture of SiO_x ($x < 2$) and SiO_2 phases, as indicated by infrared absorptance spectra of the samples. Phase separation of the SiO_x:Sm film is enhanced during annealing, resulting in an increased heterogeneity and subsequent formation of silicon nanoparticles. TOF-SIMS studies showed an almost uniform in-depth distribution of the secondary ions (Si^+, Si_2^+, O^+, SiO^+, Sm^+, SmO^+) in the SiO_x:Sm films with samarium content less than 1.0 at.%.

Optical studies of the absorption edge of the nps-Si–SiO_x:Sm nanocomposites allowed us to estimate the optical bandgap E_{go} of the silicon nanoparticles and the SiO_x matrix. The increase in the bandgap width of the *a*-Si nanoinclusions from ~1.5 eV for the as-deposited films to 1.77 eV for the films annealed at 600 °C indicates the preferential contribution of the reduction of their defectivity during heat treatment to the increase in E_{go}. The increase in E_{go} of the oxide matrix is explained by an increase in its stoichiometry index as a result of annealing, as confirmed by the IR spectra.

The light emitting properties of the SiO_x:Sm films are defined by the silicon nanoparticles formed during deposition and subsequent annealing of the samples. We believe that the strongest band with the maximum at 750 nm in the PL spectrum of the annealed film is due to exciton recombination within the Si nanoinclusions. The band with a maximum at 820 nm is associated with nps-Si surface defects at the interface with the SiO_x matrix. The long-wavelength band at 910 nm is associated with presence of crystalline or quasicrystalline nps-Si in the film. The red shift of the maximum of this band from 910 to 950 nm at increasing the annealing temperature from 600 to 700 °C, accompanied by a decrease in the PL intensity, is well explained by manifestation of the quantum-size effect due to the increase in the size of nps-Si.

Conflict of interest: The authors declare no conflict of interest.

References

1. Canham L. Introductory lecture: origins and applications of efficient visible photoluminescence from silicon-based nanostructures. *Faraday Discuss*. 2020. **222**. P. 10–81. https://doi.org/10.1039/D0FD00018C.
2. Pavesi L. Thirty years in silicon photonics: a personal view. *Front. Phys.* 2021. **9**. Art. 786028. https://doi.org/10.3389/fphy.2021.786028.
3. Iacona F., Miritello M., Boninelli S. *et al.* Light emission from silicon-based materials: From silicon nanostructures to rare earth ions. In: *Silicon Nanophotonics,* L. Khriachtchev (Ed.). Jenny Stanford Publ., 2016. P. 259–298.
4. Mazzaro R., Romano F., Ceroni P. Long-lived luminescence of silicon nanocrystals: from principles to applications. *Phys. Chem. Chem. Phys.* 2017. **19**. P. 26507–26526. https://doi.org/10.1039/C7CP05208A.
5. Melnik V.P., Popov V.G., Romanyuk B.M. *et al.* Luminescent properties of the structures with embedded silicon nanoclusters: Influence of technology, doping and annealing (Review). *SPQEO*. 2023. **26**. P. 278–302. https://doi.org/10.15407/spqeo26.03.278.
6. Frieiro J.L., López-Vidrier J., Blázquez O. *et al.* Silicon nanocrystals-based electroluminescent resistive switching device. *J. Appl. Phys.* 2019. **126**. Art. 144501. https://doi.org/10.1063/1.5119299.
7. Sarikov A. Thermodynamic theory of phase separation in nonstoichiometric Si oxide films induced by high-temperature anneals. *Nanomanufacturing*. 2023. **3**. P. 293–314. https://doi.org/10.3390/nanomanufacturing3030019.
8. Ramirez-Rios J., González-Flores K.E., Avilés-Bravo J.J. *et al.* Semiempirical two-dimensional model of the bipolar resistive switching process in Si-NCs/SiO_2 multilayers. *Nanomaterials.* 2023. **13**. Art. 2124. https://doi.org/10.3390/nano13142124.
9. Belyaev A., Maksimenko Z., Golovynskyi S. *et al.* Semiconductor nanomaterials for optoelectronics and the SPQEO journal. *SPQEO*. 2025. **28**. P. 004–009. https://doi.org/10.15407/spqeo28.01.004.
10. Zarchi M., Ahangarani S. The role of operations after the deposition on the performance of SiO_x films in optoelectronics devices. *Opt. Mater.* 2015. **46**. P. 223–227. https://doi.org/10.1016/j.optmat.2015.04.023.
11. Ahn H., Jeong J., Gu M. *et al*. Controlling photoluminescence of silicon quantum dots using pristine-nanostates formation. *Opt. Mater*. 2024. **147**. Art. 114792. https://doi.org/10.1016/j.optmat.2023.114792.
12. Falcony C., Estrada-Wiese D., De Anda J. Low temperature (< 700 °C) SiO_2 and Si-rich SiO_2 films: Short review. *J. Vac. Sci. Technol. B*. 2023. **41**. Art. 030801. https://doi.org/10.1116/6.0002531.
13. Nesheva D. Electron and neutron beam irradiation effects in homogeneous and nanostructured oxides. *ACS Omega*. 2023. **8**. P. 12603−12612. https://doi.org/10.1021/acsomega.3c00486.
14. Bratus O., Kykot A., Yukhymchuk V. *et al*. Influence of the annealing temperature on the structural and electrical properties of SiO_x(Si)&Fe_yO_z(Fe) films. *J. Phys. Chem. C.* 2025. **129**. P. 1025−1568. https://doi.org/10.1021/acs.jpcc.4c04973.
15. Mustafa D., Biggemann D., Martens J.A. *et al*. Erbium enhanced formation and growth of photoluminescent Er/Si nanocrystals. *Thin Solid Films*. 2013. **536**. P. 196–201. http://doi.org/10.1016/j.tsf.2013.03.027.
16. Beainy G., Frilay C., Pareige P. *et al*. On the interplay between Si-Er-O segregation and erbium silicate ($Er_2Si_2O_7$) formation in Er-doped SiO_x thin films. *J. Alloys Compd.* 2018. **755**. P. 55–60. https://doi.org/10.1016/J.JALLCOM.2018.04.310.
17. Nikolenko A.S., Sopinskyy M.V., Strelchuk V.V. *et al*. Raman study of Si nanoparticles formation in the annealed SiO_x and SiO_x:Er,F films on sapphire substrate. *J. Optoelectron. Adv. Mater. Rapid Commun.* 2012. **14**. P. 120–124.
18. Sopinskyy M.V., Vlasenko N.A., Lisovskyy I.P. *et al*. Formation of nanocomposites by oxidizing annealing of SiO_x and SiO_x⟨Er,F⟩ films: Ellipsometry and FTIR analysis. *Nanoscale Res. Lett.* 2015. **10**. Art. 232. https://doi.org/10.1186/s11671-015-0933-0.
19. Deopa N., Rao A.S., Choudhary A. *et al.* Photoluminescence investigations on Sm^{3+} ions doped borate glasses for tricolor w-LEDs and lasers. *Mater. Res. Bull.* 2018. **100**. P. 206–212. https://doi.org/10.1016/j.materresbull.2017.
20. Okada G., Morrell B., Koughia C. *et al.* Spatially resolved measurements of high doses in microbeam radiation therapy using samarium doped fluorophosphates glasses. *Appl. Phys. Lett.* 2011. **99**. Art. 121105. https://doi.org/10.1063/1.3633102.
21. Michailovska K.V., Indutnyi I.Z., Shepeliavyi P.E. *et al*. Samarium–induced enhancement of SiO_x decomposition and Si nanocrystals formation *Appl. Nanosci.* 2023. **13**. P. 4779–4786. https://doi.org/10.1007/s13204-022-02617-0.
22. Michailovska K.V., Indutnyi I.Z., Shepeliavyi P.E. *et al*. Formation of silicon nanocomposites by annealing of $(SiO_x/Sm)_n$ multilayers: Luminescence, Raman and FTIR studies. *Appl. Nanosci.* 2023. **13**. P. 7187–7194. https://doi.org/10.1007/s13204-023-02887-2.
23. Michailovska K.V., Indutnyi I.Z., Shepeliavyi P.E. *et al*. Luminescent and Raman study of nanostructures formed upon annealing of SiO_x:Sm films. *SPQEO*. 2023. **26**. P. 068–075. https://doi.org/10.15407/spqeo26.01.068.
24. Galeener F.L. Band limits and the vibrational spectra of tetrahedral glasses. *Phys. Rev. B*. 1979. **19**. P. 4292–4297. https://doi.org/10.1103/PhysRevB.19.4292.
25. Okada T., Onta E. Visible photoluminescence from evaporated SiO_x thin films. *Jpn. J. Appl. Phys.* 2002. **41**. P. 6413–6416. https://doi.org/10.1143/JJAP.41.6413.

26. Li S., Silver S.J., El-Shall M.S. Surface oxidation and luminescence properties of weblike agglomeration of silicon nanocrystals produced by a laser vaporization-controlled condensation technique. *J. Phys. Chem. B.* 1997. **101**. P. 1794–1802. https://doi.org/10.1021/jp963192m.
27. Yi L.X., Heitmann J., Scholz R., Zachrias M. Phase separation of thin SiO layers in amorphous SiO/SiO_2 superlattices during annealing. *J. Phys.: Condens. Matter.* 2002. **15**. P. S2887–S2895. https://doi.org/10.1088/0953-8984/15/39/012.
28. Zanatta A.R. Coexistence of $Sm^{3+}$and Sm^{2+} ions in amorphous SiO_x: origin, main light emission lines and excitation-recombination mechanisms. *Opt. Mater. Express.* 2016. **6**. P. 2109–2117. https://doi.org/10.1364/OME.6.002108.
29. Metz P.W., Marzahl D.T., Majid A. *et al.* Efficient continuous wave laser operation of Tb^{3+}-doped fluoride crystals in the green and yellow spectral regions. *Laser Photonics Rev*. 2016. **10**. P. 335–344. https://doi.org/10.1002/lpor.201500274.
30. Demoulin R., Khomenkova L., Labbe C. *et al.* Correlation of luminescence measurements to the structural characterization of Pr^{3+}-doped $HfSiO_x$. *J. Lumin*. 2021. **235**. Art. 118004. https://doi.org/10.1016/j.jlumin.2021.118004.
31. Hernández Simón Z.J., Luna López J.A., de la Luz A.D.H. *et al.* Spectroscopic properties of nc-Si in SiO_x films using HFCVD. *Nanomaterials.* 2020. **10**. Art. 1415. https://doi/10.3390/nano10071415.
32. Tauc J. Optical properties of amorphous semiconductors, in: J. Tauc (Ed.) *Amorphous and Liquid Semiconductors*. Plenum Press, London and New York, 1974. P. 159–220.
33. Cody G.D., Tiedje T., Abeles B. *et al.* Disorder and the optical-absorption edge of hydrogenated amorphous silicon. *Phys. Rev. Lett*. 1981. **47**. P. 1480–1483. https://doi.org/10.1103/PhysRevLett.47.1480.
34. Park N.-M, Choi C.-J., Seong T.-Y., Park S.-J. Quantum confinement in amorphous silicon quantum dots embedded in silicon nitride. *Phys. Rev. Lett.* 2001. **86**. P. 1355–1357. https://doi.org/10.1103/PhysRevLett.86.1355.
35. Jambois O., Rinnert H., Devaux X., Vergnat M. Influence of the annealing treatments on the luminescence properties of SiO/SiO_2 multilayers. *J. Appl. Phys.* 2006. **100**. Art. 123504. https://doi.org/10.1063/1.2402976.
36. Indutnyy I.Z., Lisovskyy I.P., Masunov D.O. *et al.* Optical study of thermally induced phase separation in evaporated SiO_x films. *SPQEO*. 2004. **7**. P. 161–167. https://doi.org/10.15407/spqeo7.02.161.
37. Zhuravlev K.S., Gilinsky A.M., Kobitsky A.Y. Mechanism of photoluminescence of Si nanocrystals fabricated in a SiO_2 matrix. *Appl. Phys. Lett.* 1998. **73**. P. 2962–2964. https://doi.org/10.1063/1.122644.
38. Ossicini S., Degoli E., Luppi M., Magri R. Si nanostructures embedded in SiO_2: electronic and optical properties. *Proc. SPIE*. 2002. **4808**. P. 73–84. https://doi.org/10.1117/12.452043.

Authors and CV

Katerina V. Michailovska, PhD in Physics and Mathematics, Senior Researcher at the V. Lashkaryov Institute of Semiconductor Physics, NAS of Ukraine. Authored 170 publications, 15 patents, and 1 monograph. The area of her scientific interests is physics (optic, luminescence) of thin-film semiconductor structures and nanosized systems based on them.
http://orcid.org/0000-0001-6088-7123

Petro E. Shepeliavyi
4.02.1950 – 5.05.2024
PhD in Technical Sciences, worked as a Senior Researcher at the V. Lashkaryov Institute of Semiconductor Physics, NAS of Ukraine.
His interests included inorganic resists and their application in lithography, holography, optical engineering, information recording, absorbing metal-dielectric coatings, *etc*. Author of more than 250 publications and 40 author's certificates and patents.
http://orcid.org/0000-0002-4119-1099

Vitalii K. Lytvyn, PhD in Technical Sciences, Researcher at the Department of Biochemosensorics of the V. Lashkaryov Institute of Semiconductor Physics, NASU. Authored and co-authored 40 publications and 9 patents. His research interests include plasmon-enhanced fluorescence, nanotechnology, electronics, and development of random and highly ordered high-conductive nanostructure arrays for plasmonic and biotechnological applications.
E-mail: lytvet@ukr.net,
https://orcid.org/0000-0003-1241-4457

Oleksandr Dubikovskyi, PhD in Physics and Mathematics, Researcher at the Department of Ion-Beam Engineering and Structural Analysis at the V. Lashkaryov Institute of Semiconductor Physics, NASU. Author of more than 20 publications. The main directions of his scientific activity are ion-beam modification and mass-spectrometry of semiconductor structures. E-mail: dubikovsky_o@ukr.net,
https://orcid.org/0000-0002-1504-8440

Viktor A. Dan'ko, Doctor of Sciences in Physics and Mathematics, Leading Researcher at the V. Lashkaryov Institute of Semiconductor Physics, NAS of Ukraine. His main research activity is in the field of optics of thin films, photostimulated processes in thin film structures, nanoparticles and nanostructures, and interference lithography. He is the author of more than 170 publications and patents.
E-mail: danko-va@ukr.net,
http://orcid.org/0000-0001-8106-3182

Ivan Z. Indutnyi, Doctor of Sciences in Physics and Mathematics, Professor, Chief Researcher at the V. Lashkaryov Institute of Semiconductor Physics, NAS of Ukraine. His main research activity is in the field of optics of thin films, photostimulated processes in solids and on their surfaces, nanoparticles and nanostructures, interference lithography, plasmonics and sensing. Author of more than 300 publications and 35 author's certificates and patents. E-mail: indutnyy@isp.klev.ua,
http://orcid.org/0000-0002-7088-744X

Authors contributions

Michailovska K.V.: conceptualization, project administration, methodology, investigation, formal analysis, visualization, writing – original draft, writing – review and editing.
Shepeliavyi P.E.: conceptualization, methodology, investigation.
Lytvyn V.K.: methodology, investigation, visualization.
Dubikovskyi O.V.: methodology, investigation, visualization.
Dan'ko V.A.: investigation, resources, funding acquisition.
Indutnyi I.Z.: supervision, methodology, writing – review and editing.
Sopinskyy M.V.: data curation, formal analysis, visualization, writing – original draft, writing – review and editing.

Оптичні та світловипромінювальні властивості кремнієвих наноструктур на основі плівок SiO_x, модифікованих самарієм

К.В. Михайловська, П.Є. Шепелявий, В.К. Литвин, О.В. Дубіковський, В.А. Данько, І.З. Індутний, М.В. Сопінський

Анотація. Досліджено склад, оптичні та люмінесцентні властивості плівок SiO_x:Sm, отриманих термічним випаровуванням у вакуумі порошкової суміші (SiO + Sm), Sm ~ 1 ваг.%. Дослідження елементних профілів за допомогою часопролітної мас-спектроскопії вторинних іонів виявило майже рівномірний розподіл основних елементів (іонів Si^+, Si_2^+, O^+, SiO^+), а також іонів Sm^+ і SmO^+ по глибині. ІЧ-спектри показали більшу мікроструктурну неоднорідність матриці SiO_x порівняно з нелегованими плівками SiO_x, отриманими за аналогічного режиму осадження. Подальша термообробка у вакуумі при 500–700 °C підвищує ступінь неоднорідності зразків. Значення оптичної забороненої зони 1,5 еВ до та 1,77 еВ після відпалу при 600 °C плівок SiO_x:Sm, визначені методом Тауца, добре корелюють з літературними даними для аморфного кремнію та нановключень Si у матриці SiO_2 відповідно. Вимірювання спектрів фотолюмінесценції та їх аналіз показали, що легування плівок SiOx самарієм стимулює їх розпад, а термообробка при температурі відпалу ≥ 600 °C утворює в оксидній матриці наночастинки Si, які проявляють квантово-розмірний ефект.

Ключові слова: наночастинки кремнію, SiO_x, нанокомпозит, самарій, рідкісноземельні елементи, лантаноїди, люмінесценція.